Received: 25 December 2025 | Revised: 13 March 2026 | Accepted: 6 May 2026

DOI: 10.1002/ame2.70233

ORIGINAL ARTICLE

Identification and validation of fecal complement component 3 and fibronectin as potential biomarkers for monitoring disease activity in ulcerative colitis based on a mouse model

Yangyun Guo[1,2] | Ziheng Yan[2] | Jingyu Ye[2] | Ruifu Yang[2] | Yajun Song[2] | Hui Yue[1] | Yong Zhao[2]

[1]School of Basic Medical Sciences, Mudanjiang Medical University, Heilongjiang, China

[2]State Key Laboratory of Pathogen and Biosecurity, Academy of Military Medical Sciences, Beijing, China

Correspondence
Yong Zhao, State Key Laboratory of Pathogen and Biosecurity, Academy of Military Medical Sciences, Beijing, China.
Email: zhaoyong179@139.com

Hui Yue, School of Basic Medical Sciences, Mudanjiang Medical University, Heilongjiang, China.
Email: yuehui1982@163.com

Funding information
National Natural Science Foundation of China, Grant/Award Number: 32394054

Abstract

Background: Ulcerative colitis (UC) is a typical inflammatory bowel disease requiring long-term management. Although fecal calprotectin (FC) is widely employed for assessing disease activity, it is still considered insufficient as a standalone tool. New biomarkers are needed to better predict risk and comprehensively reflect biological pathways. This study aimed to identify potential fecal biomarkers to monitor disease activity in UC.

Methods: C57BL/6J mice were exposed to dextran sulfate sodium (DSS) treatment for 7 days. Feces were collected and subjected to proteomic analysis and enzyme-linked immunosorbent assay (ELISA). Mouse colon tissues were subjected to histopathological and immunofluorescence analyses. The correlations between the selected fecal proteins and disease severity were evaluated and compared with FC.

Results: Proteomic analysis revealed increases in fecal complement component 3 (C3) and fibronectin (FN) in the DSS group. Next, we measured fecal C3 and FN levels in mice using ELISA. Significant elevation in C3 and FN levels was observed as early as day 1 after DSS treatment, preceding the increase in FC. Both fecal C3 and FN demonstrated significant correlations with disease activity, with C3 exhibiting a stronger correlation than FC. Using immunofluorescence, we observed distinct C3 and FN expressions in both the colonic tissues and the intestinal lumen.

Conclusion: These findings demonstrate that fecal C3 and FN are promising candidate biomarkers for monitoring UC disease activity, and their utility requires further validation in other colitis models and human cohorts.

KEYWORDS
complement component 3 (C3), disease activity, fibronectin, mouse model, ulcerative colitis

1 | INTRODUCTION

Ulcerative colitis (UC) is a chronic inflammatory bowel disease with an increasing global incidence in recent years. Its clinical course is typically characterized by alternating active phases and remission phases. Major symptoms, such as bloody stools, usually occur during the active phase.[1] Dynamic monitoring disease activity is crucial for the clinical treatment and management of UC patients.[2] Despite being the gold standard, endoscopy and tissue biopsy are invasive, expensive, and limited for dynamic evaluation.[3] Therefore, there is an immediate need to develop efficient and noninvasive tools for monitoring intestinal health in UC patients.

Fecal calprotectin (FC) has proven invaluable in assessing disease activity for UC patients.[4,5] In contrast to common blood measurements, FC measurement offers a convenient and noninvasive sampling process, and provides a direct indication of gut inflammation.[6] The onset and progression of UC involve multiple pathophysiological processes, such as disruption of the mechanical barrier, immune dysregulation, and gut microbiota imbalance.[7] However, FC mainly focuses on reflecting the level of neutrophil-related inflammation and is unable to fully reflect the extent of intestinal damage in UC. Apart from FC (along with lactoferrin), there still remains a lack of reliable fecal biomarkers that can reflect these pathophysiological processes across multiple dimensions.[8,9]

Currently, researchers have employed high-throughput proteomic approaches to profile the fecal proteome of UC patients or murine models.[10] Several potential biomarkers have been successfully identified.[11] A few biomarkers, such as lipocalin 2 (LCN2), have been preliminarily validated in clinical cohorts, yet their value remains no better than FC.[12,13] Most candidates still lack rigorous validation and require to be tested further.

Complement component 3 (C3) is the most abundant and core component in the complement system, participating in the clearance of immune complexes, release of inflammatory mediators, and elimination of pathogens.[14] C3 is primarily synthesized in the liver and circulates in the bloodstream. Recent studies, however, have shown that it can also be produced locally by cells in the intestinal tissue (primarily by stromal cells).[15] And its expression is significantly upregulated during enteric infections.[16] Fibronectin (FN) is an essential extracellular matrix (ECM) protein vital for maintaining the mechanical barrier. It directly contributes to functional reconstruction during tissue repair (including intestinal injury).[17] In clinical practice, changes in the plasma concentrations of C3 and FN serve as important biomarkers for assessing systemic inflammation and tissue repair status, respectively.[14,17] However, the direct correlation between their fecal levels and the extent of intestinal tissue damage or disease activity has been seldom reported.

In this study, a UC mouse model was established using dextran sulfate sodium (DSS) treatment. Subsequent high-throughput proteomic analysis of fecal samples revealed a significant enrichment of complement C3 and FN in the DSS group. This elevation was further validated using enzyme-linked immunosorbent assay (ELISA). Results suggested that fecal C3 and FN levels were elevated early after DSS treatment, preceding the increase in FC. Moreover, both fecal C3 and FN demonstrated significant correlations with disease activity, with C3 exhibiting a stronger correlation than FC. These findings indicate that fecal C3 and FN are promising candidate biomarkers for monitoring UC disease activity, and their utility requires further validation in other colitis models and human cohorts.

2 | MATERIALS AND METHODS

2.1 | Establishment of the DSS-induced UC mouse model

Specific pathogen-free (SPF)-grade 8-week-old female C57BL/6J mice were purchased from Vital River Laboratory Animal Technology Co., Ltd. (Beijing, China). A batch of 70 mice were first randomly divided into seven cohorts (days 1–7, $n = 10$ per cohort). Within each cohort, mice were further randomly assigned to either a DSS or a normal control (NC) subgroup ($n = 5$ per subgroup). Therefore, across all cohorts, 35 mice were in the DSS group and 35 in the NC group. Mice were housed under SPF conditions with free access to food and water. The experimental environment was maintained under a temperature of 23 ± 2°C and a relative humidity of $50\% \pm 10\%$. All mice were acclimatized for 1 week to adapt to the experimental settings. All mice were housed individually in cages. The mice in the DSS group were allowed to freely drink a 3% DSS (0216011080, MP Biomedicals LLC, San Antonio, CA, USA) aqueous solution, which was replaced every 2 days for 7 days. The mice in the NC group were allowed to freely drink distilled water.

Throughout the modeling period, daily fecal samples from each surviving mouse were collected and stored at −80°C for subsequent analyses. The general condition of the mice, including mental status and coat appearance, was systematically and continuously monitored throughout the experiment. A blind design was adopted for mouse body weight measurement, fecal occult blood testing, fecal morphology grading, and disease activity index (DAI) calculation. The DAI was calculated according to the commonly established criteria (Table S1).

Another batch of C57BL/6J mice ($N = 12$) were randomly assigned to the NC and DSS groups (six mice per group). Mice in the DSS group received 3% DSS in drinking water, following the same protocol as the first batch. On day 7, fecal samples from both groups were collected for proteomic analysis.

2.2 | Hematoxylin–eosin and immunofluorescence staining

Mice from the day 1, day 3, day 5, and day 7 cohorts were euthanized for colon tissue collection on days 1, 3, 5, and 7 of the experiment, respectively, after clinical observation and fecal sample collection. The collected tissues were immediately fixed in 4% paraformaldehyde

for 24 h; the tissues were then subjected to gradient dehydration, xylene clearing, and paraffin embedding to prepare paraffin blocks. These blocks were sectioned into 5-μm-thick slices using a rotary microtome; the sections were then mounted on slides and incubated at 60°C for 2 h.

The sections were stained with hematoxylin–eosin (HE). After staining, the samples were observed under a light microscope. Histopathological score (HS) was analyzed based on ulcer number, epithelial cell morphological changes, and the degree of inflammatory cell infiltration; this was performed by Wuhan Servicebio Technology Co., Ltd. (Wuhan, Hubei, China) in a blind manner. Quantitative scoring was conducted according to the commonly employed criteria (Table S2).

A brief description of the immunofluorescence method for colon tissue is as follows. After dewaxing and rehydration of the paraffin sections, antigen retrieval was performed by heating the sections in EDTA antigen retrieval buffer (pH 9.0) at 100°C for 25 min. After the sections were cooled to room temperature, they were sequentially treated with 3% hydrogen peroxide to block endogenous peroxidase activity and 5% bovine serum albumin to block nonspecific binding sites. The sections were then incubated with three specific antibodies—mucin-2 (MUC2, GB11344, Wuhan Servicebio Technology Co., Ltd), FN (GB114491, Wuhan Servicebio Technology Co., Ltd), and C3 (ab200999, Abcam plc, Cambridge, UK)—and with a horseradish peroxidase–conjugated goat anti-rabbit IgG secondary antibody. Nuclear counterstaining was performed using 4′,6-diamidino-2-phenylindole, and nonspecific autofluorescence was quenched using an autofluorescence quencher. Finally, the sections were mounted using an antifade mounting medium and coverslipped. Images were obtained and analyzed using a laser scanning confocal microscope.

2.3 | Proteomic analysis of fecal samples

2.3.1 | Protein extraction and digestion

Fecal samples (six biological replicates for each group) were collected, rapidly frozen in liquid nitrogen, and ground into a fine powder. An appropriate amount of powder was transferred to a 1.5-mL centrifuge tube and mixed with lysis buffer for complete lysis. After sonication on ice for 5 min, the mixture was centrifuged at 15 000*g* and 4°C for 10 min; the supernatant was collected, and protein concentration was determined. A 100-μg aliquot of the protein solution was adjusted to 200 μL with 8 mol/L urea, supplemented with DL-dithiothreitol (final concentration: 5 mmol/L), and incubated at 37°C for 45 min for reduction. Subsequently, iodoacetamide (final concentration: 11 mmol/L) was added, and the sample was incubated in the dark at room temperature for 15 min for alkylation. Next, 800 μL of 25 mmol/L ammonium bicarbonate solution and 2 μL of trypsin were added; the mixture was incubated overnight at 37°C for peptide digestion. The digested peptides were adjusted to pH 2 using 20% trifluoroacetic acid and purified using reversed-phase C18 column chromatography. Peptide concentration was quantified using the Pierce Quantitative Peptide Assay Kit (23275, Thermo Fisher Scientific Inc., MA, USA).

2.3.2 | Liquid chromatography–tandem mass spectrometry analysis

Peptide separation was performed on a Vanquish Neo UHPLC nano-liquid chromatography system (Thermo Fisher Scientific Inc.) using a trap–elute dual-column mode. The trap column was a PepMap Neo Trap Cartridge (300 μm × 5 mm, 5 μm), and the analytical column used was an Easy-Spray PepMap Neo UHPLC column (150 μm × 15 cm, 2 μm). Mobile phase A consisted of 0.1% formic acid in water, and mobile phase B consisted of 0.1% formic acid in 100% acetonitrile. The peptide sample (200 ng) was loaded and separated at a flow rate of 2.5 μL/min over an 8-min gradient.

Mass spectrometry (MS) analysis was conducted on an Orbitrap Astral high-resolution mass spectrometer (Thermo Fisher Scientific Inc.) in positive ion mode with data-independent acquisition (DIA). Full MS scans were acquired over a range of 380–980 *m/z* at a resolution of 240 000 (at 200 *m/z*), with a normalized automatic gain control (AGC) target of 500% and a maximum injection time of 5 ms. DIA tandem mass spectrometry (MS/MS) employed 299 scanning windows with an isolation window of 2 Th, a higher-energy C-trap dissociation fragmentation at 25% energy, a normalized AGC target of 50%, and a maximum injection time of 3 ms.

2.3.3 | Data processing and analysis

Raw MS data were analyzed using DIA-NN software (version 1.8.1) using a library-free approach to search the UniProt mouse database. Peptide and protein identification was performed with the false discovery rate (FDR) controlled at less than or equal to 1% using the built-in target-decoy search approach. Differentially expressed proteins were selected based on a fold-change threshold of ≥ 1.5 or ≤ 0.667 and an adjusted *p*-value of ≤ 0.05. FDR correction was applied using the Benjamini–Hochberg method. Functional annotations, including Gene Ontology (GO) and Kyoto Encyclopedia of Genes and Genomes (KEGG) pathways, were conducted for all identified proteins and differentially expressed proteins. Enrichment analysis was also performed on differentially expressed proteins to determine their enrichment trends in specific functional categories and clarify the associated physiological functions.

2.3.4 | Protein selection criteria

To select potential candidates from the differentially expressed proteins, we applied both inclusion and exclusion criteria. Inclusion criteria were (1) evidence of local intestinal synthesis and involvement in inflammation or tissue repair, (2) involvement in

pathways significantly enriched by KEGG or GO analyses, and (3) evidence of transcriptional upregulation in the inflamed intestine. Exclusion criteria were (1) proteins previously reported and evaluated as biomarkers of intestinal inflammation and (2) proteins without commercial detection kits.

2.4 | Quantification of selected proteins using ELISA

Fecal samples tested using ELISA were obtained from each independent cohort on its assigned sampling day: the day 1 cohort on day 1, the day 2 cohort on day 2, and so on through the day 7 cohort on day 7. Fecal sample (0.1 g) was weighed and placed in a microcentrifuge tube; 1.5 mL of precooled phosphate-buffered saline was added, and the mixture was ground. All samples were subjected to low-temperature centrifugation at 8000*g* and 4°C for 5 min, and the supernatants were collected. After appropriate dilution, the concentration of candidate proteins in the supernatant was, respectively, measured using a set of commercial ELISA kits, including the complement C3 ELISA Kit (EM0319, Wuhan Fine Biotech Co., Ltd., Wuhan, Hubei, China), FN ELISA Kit (EM0079, Wuhan Fine Biotech Co., Ltd), FC ELISA Kit (EM1620, Wuhan Fine Biotech Co., Ltd), Muc-2 ELISA Kit (EK2156, Signalway Antibody LLC, MD, USA), and Reg 3γ ELISA Kit (SEE676Mu, Cloud-Clone Corp., Wuhan, Hubei, China). All measurements were performed using the manufacturer's instructions. We set the threshold for each protein using data from mice in all the control groups ($N=35$), calculating it as the mean plus two standard deviations (mean ± 2 SD). The effect size (Cohen's *d*) was calculated using the formula:

$$d = \frac{\overline{x_1} - \overline{x_2}}{S_{\text{pooled}}}$$

where the pooled standard deviation (s_{pooled}) is defined as

$$s_{\text{pooled}} = \sqrt{\frac{(n_1 - 1){s_1}^2 + (n_2 - 1){s_2}^2}{n_1 + n_2 - 2}}$$

Here $\overline{x_1}$ and $\overline{x_2}$ represent the means of the two groups, s_1 and s_2 represent the standard deviations of the two groups, and n_1 and n_2 represent the sample sizes of the two groups.

2.5 | Statistical methods

Data analyses were conducted using GraphPad Prism, version 10.0 (San Diego, CA, USA). Prior to parametric testing, Shapiro–Wilk test was used to verify data normality. For data conforming to a normal distribution, unpaired Student's *t*-tests were used for two-group comparisons. For nonnormally distributed data, the nonparametric Mann–Whitney *U*-test was applied instead.

For comparisons of continuous variables across multiple groups, one-way analysis of variance (ANOVA) was used; post hoc pairwise comparisons were implemented using Dunnett's test, with significance established at $p<0.05$. Two-way ANOVA was employed to assess the effects of treatment and time on mouse body weight and DAI scores; post hoc pairwise comparisons were performed using Šídák's multiple comparison test, with a significance level set at $\alpha=0.05$.

Spearman's rank correlation analysis was performed to explore potential associations between fecal protein levels and disease severity (DAI score and HS) from the same individual. Differences were considered statistically significant when $p<0.05$. Williams test, along with Bonferroni correction, was employed to compare two nonindependent Spearman's correlation coefficients. Sample size was estimated using PASS 2021 software (NCSS, Kaysville, UT, USA) for Spearman's correlation ($\rho=0.5$, power = 0.8, $\alpha=0.05$, 2000 simulations), yielding a required minimal sample size of 34.

3 | RESULTS

3.1 | Establishment and evaluation of the DSS-induced UC mouse model

Figure 1A-E shows that mice in the DSS group exhibited significant weight loss, colon shortening, and elevated disease activity compared to the control group. Specifically, the DSS group exhibited a significantly higher DAI value ($p<0.0001$) than the controls on the third day with 3% DSS treatment. HE staining analysis revealed that the HS of the DSS group increased significantly starting from day 5 (Figure 1F). Focal ulcers and epithelial sloughing appeared on day 5; by day 7, the lesions had progressed to extensive ulcers with significant loss of intestinal glands and inflammatory cell infiltration.

3.2 | Fecal proteomic analysis and differentially expressed protein screening

Fecal proteins were extracted on day 7 from both the DSS and control groups ($n=6$ per group) and analyzed using liquid chromatography-MS/MS. A clear separation between the DSS and control groups was observed in the principal component analysis (PCA) plot (Figure 2A), showing distinct global protein expression profiles between the groups. A total of 1142 differentially expressed proteins were selected according to the predefined thresholds (fold change ≥ 1.5 or ≤ 0.667, and adjusted *p*-value ≤ 0.05) (Figure 2B). The complete dataset is available in Data S1. Specifically, 977 proteins were significantly upregulated in the DSS group, among which a subset exhibited more significant upregulation than FC. Among the most upregulated proteins, we observed several key complement components, including complement factor H (CFH), complement factor B (CFB), and C3. Other highly elevated proteins included hemoglobin, apolipoprotein, LCN2, serotransferrin, integrin, and FN (Figure 2C). Based on the predefined selection criteria in the Materials and Methods section, fecal C3 and FN were identified as candidate proteins for further validation.

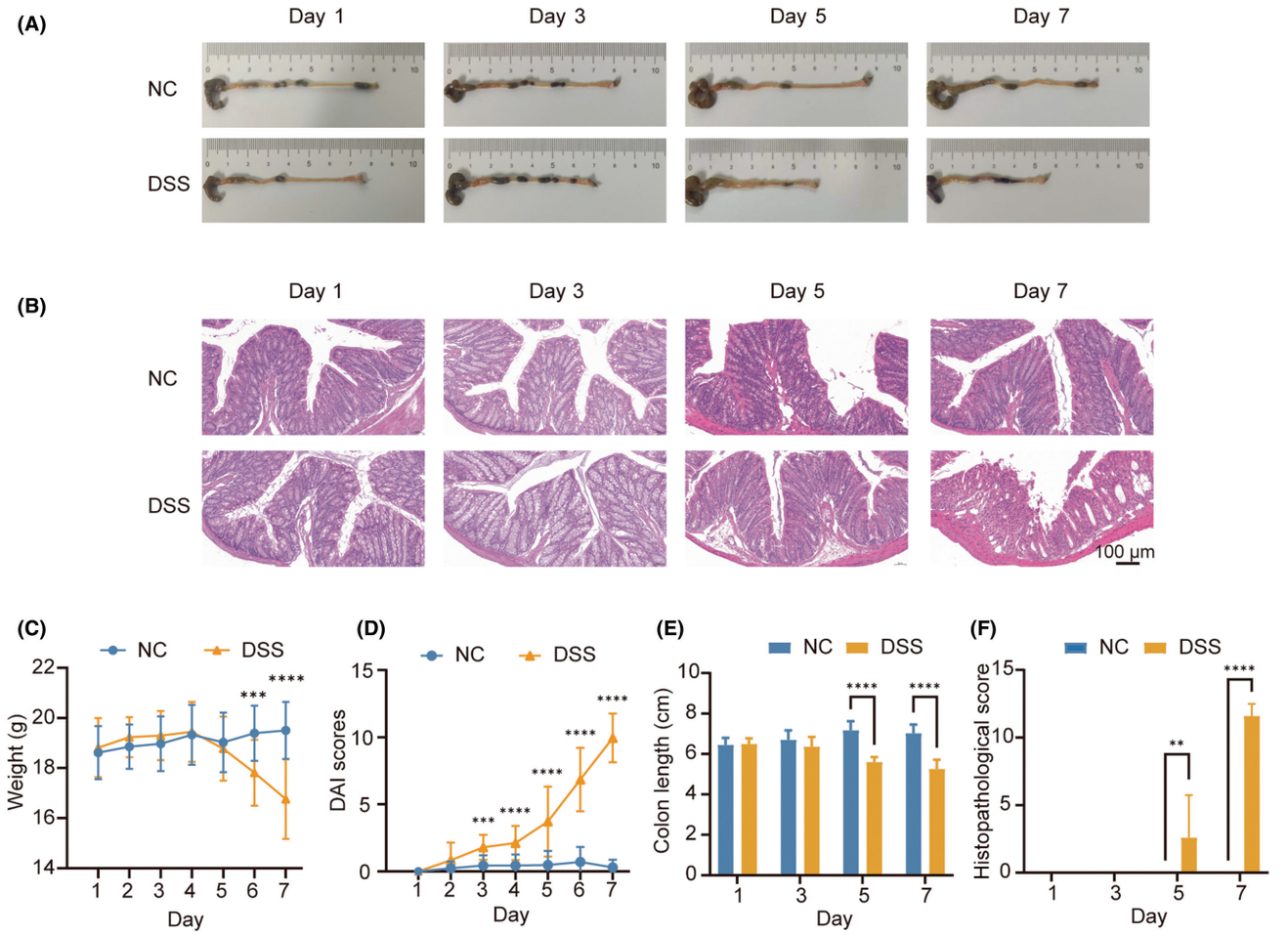

FIGURE 1 Establishment and assessment of the DSS (dextran sulfate sodium)-induced UC (ulcerative colitis) mouse model. (A, B) Representative colon image and HE (hematoxylin–eosin)–stained colon tissue from NC (normal control) and DSS-treated mice on days 1, 3, 5, and 7. (C, D) Changes in body weight and DAI (disease activity index) scores of mice during modeling. This experiment began with $n = 35$ mice per group. At each tissue sampling timepoint, five mice per group were euthanized. Data points represent measurements from all surviving mice on each day. (E, F) Changes in colon length and histopathological score of mice on days 1, 3, 5, and 7. Data are presented as mean ± SD (standard deviation), with five mice per group per timepoint. $^{**}p < 0.01$, $^{***}p < 0.001$, and $^{****}p < 0.0001$.

Complement C3 was selected as a candidate due to its local synthesis by intestinal epithelial cells and its established association with intestinal inflammation.[15,16] Moreover, our KEGG pathway analysis revealed significant enrichment of the complement activation cascade (Figure S1), indicating systemic activation of the complement pathway rather than merely the enrichment of individual complement components. This finding is consistent with previous reports; transcriptional activation and upregulation of the complement system in intestinal tissue have been demonstrated in both DSS-induced colitis models and UC patients.[18]

FN is a major component of the intestinal ECM and contributes to tissue integrity and repair.[17] Previous studies have shown that intestinal FN transcription could be upregulated during colitis.[19] Particularly, FN has been observed to shed from the intestinal tissue under inflammatory conditions.[20] This observation is consistent with our GO analysis, which identified a significant enrichment of extracellular and collagen-containing ECM proteins in the feces of UC mice (Figure S1).

3.3 | Quantification of selected fecal proteins using ELISA

From proteomic analysis, we selected fecal C3 and FN as two potential candidates. In addition, we included MUC2, a major structural component of the intestinal mucus layer,[21] and regenerating islet-derived protein 3γ (Reg 3γ), an antimicrobial peptide present in the mucus layer,[22] as two further candidates. To analyze stage-specific changes in fecal protein levels during UC progression, we used a multi-timepoint independent cohort design and quantified the proteins using ELISA. In DSS-treated mice, fecal C3 levels were significantly elevated compared to controls from day 1 onward and exceeded the predefined threshold, while FC levels did not surpass the threshold until the day 3 cohort (Figure 3A,B). An early increase in FN was also observed, despite considerable interindividual variability among the DSS-treated mice (Figure 3C). MUC2 significantly increased in the DSS-treated mice of day 1 and day 2 cohorts compared to controls but returned to a level comparable to controls in later cohorts

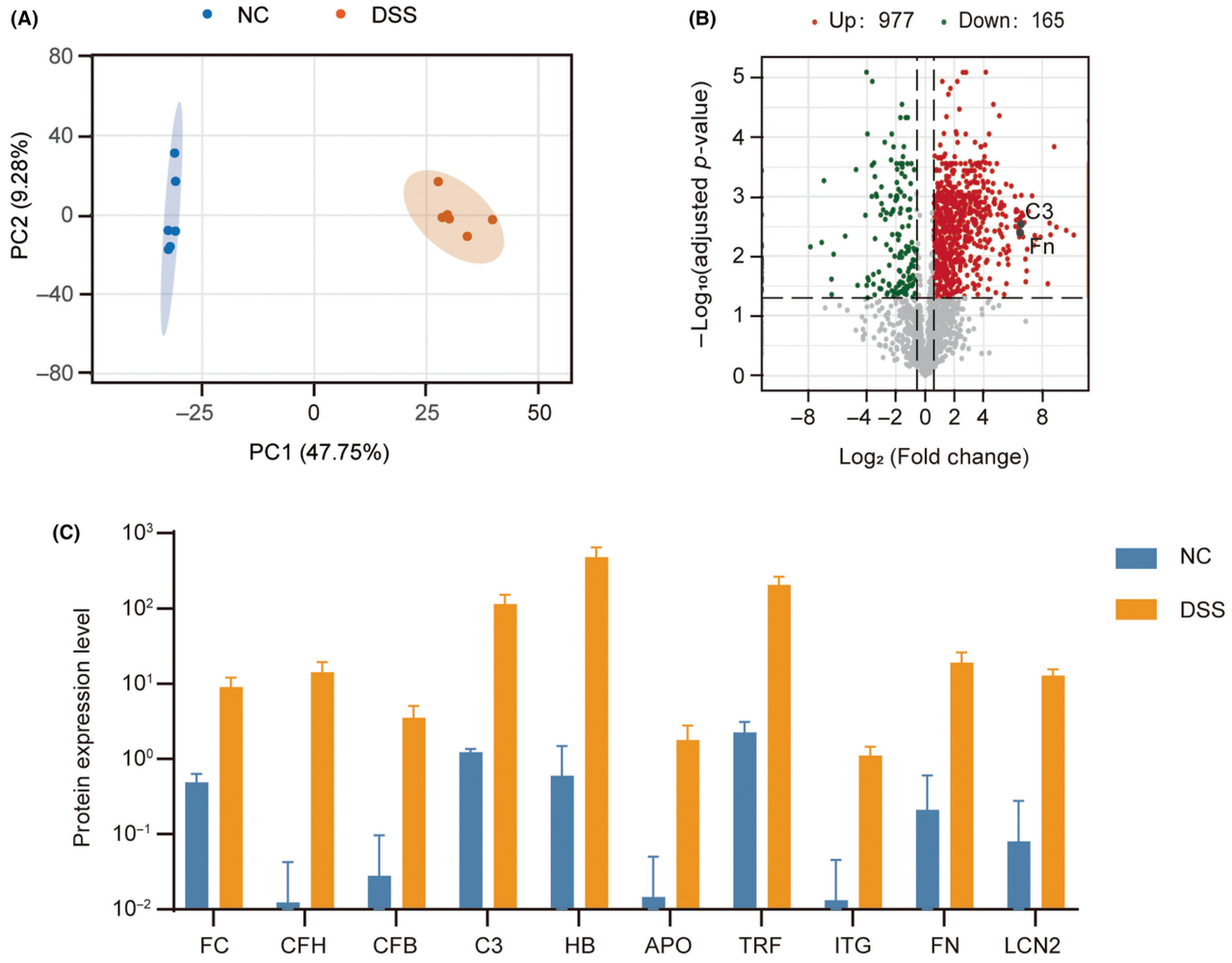

FIGURE 2 Fecal proteomic analysis and differential protein screening in UC (ulcerative colitis) mice. (A) PCA score plot. Data points correspond to individual biological replicates ($n=6$ per group). (B) Volcano plot of the differentially expressed proteins. The horizontal axis represents $\log_2$ (fold change), and the vertical axis represents $-\log_{10}$ (p-value). Dots of different colors correspond to upregulated and downregulated differentially expressed proteins. (C) Protein expression levels of the highly upregulated proteins. The horizontal axis represents the proteins, and the vertical axis represents the relative protein expression levels.

(Figure 3D). Reg 3γ levels showed no significant changes in response to DSS treatment in any cohort (Figure 3E). Collectively, these results suggest that the elevations in fecal C3 and FN occurred earlier than the increase in FC after DSS treatment.

In the DSS group, the peak concentrations of fecal FN and C3 were ~500- and ~30-fold higher than the controls, respectively (Figure 3F). In contrast, the peak concentration of FC increased only threefold, exhibiting a much lower response intensity than either FN or C3. The effect sizes (Cohen's d) for FN ($d=1.680$) and C3 ($d=1.670$) were larger than those for FC ($d=0.491$), also suggesting that they are more responsive to DSS challenge.

3.4 | Correlations of the selected fecal proteins with UC disease severity

We further analyzed the correlation between disease severity (DAI and HS) and the levels of fecal C3, FN, and FC, respectively. Spearman's rank correlation analysis revealed that fecal C3 exhibited the strongest positive correlation with DAI ($r=0.6635$, $p<0.0001$), followed by FC ($r=0.4016$, $p=0.0168$) and FN ($r=0.3638$, $p=0.0317$) (Figure 4A–C). Subsequently, pairwise comparisons were conducted among these three correlation coefficients. The result indicated that the correlation between fecal C3 and DAI was significantly stronger than that between FC and DAI (corrected $p=0.0300$). In contrast, no statistically significant difference was found between the strength of correlation for FN and DAI versus that for FC and DAI (corrected $p>0.05$). These results demonstrate that, among the biomarkers tested, fecal C3 exhibits the strongest association with disease activity.

In assessing correlations with histological severity, we found that fecal C3 exhibited the highest correlation with the HS ($r=0.6492$, $p=0.002$), followed by FC ($r=0.5375$, $p=0.0145$) and FN ($r=0.3771$, $p=0.1012$) (Figure 4D–F). However, the correlation of C3 with the HS was not significantly stronger than that of FC ($p>0.05$) using the Williams' test.

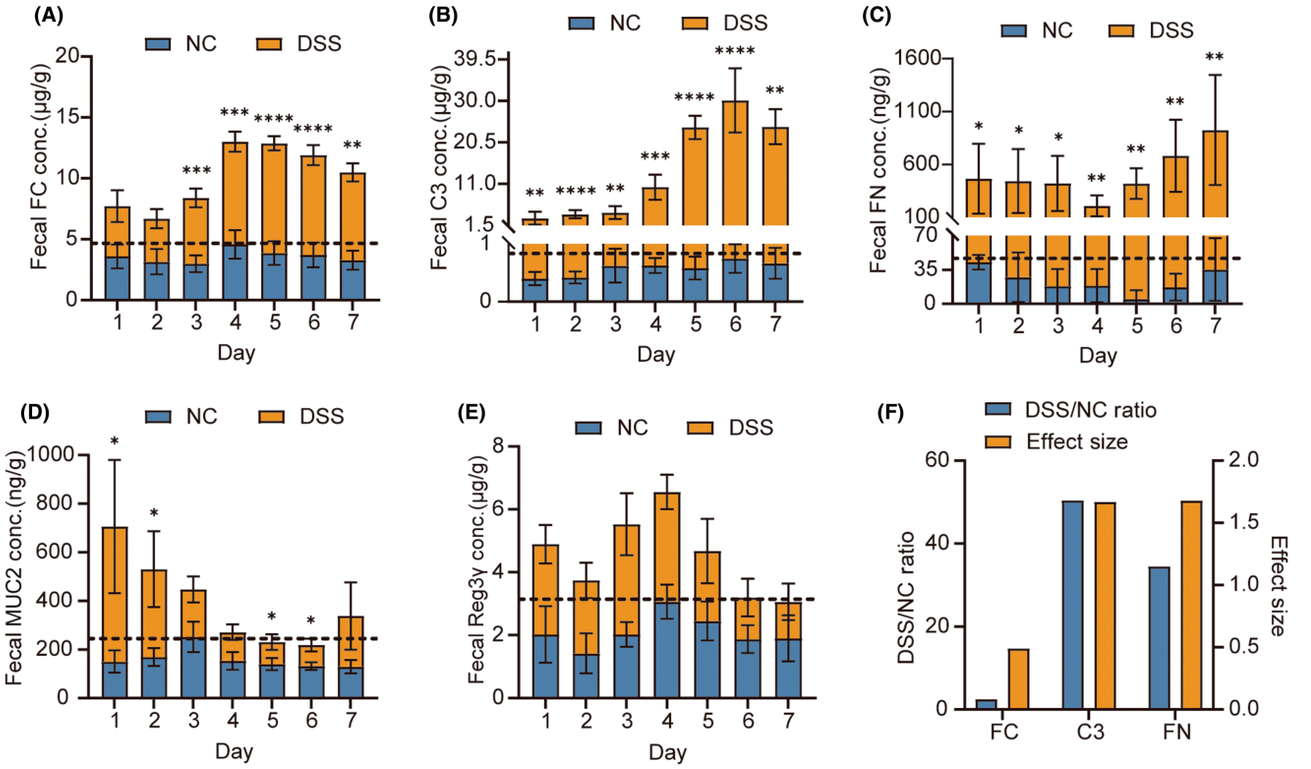

FIGURE 3 Quantitative measurements of fecal protein levels in UC (ulcerative colitis) mice. (A–E) Levels of FC (fecal calprotectin), C3 (component 3), FN (fibronectin), MUC2 (mucin-2), and Reg 3γ (regenerating islet-derived protein 3γ) measured in fecal samples from independent cohorts of mice on their assigned sampling day. Data are presented as mean ± SD (standard deviation), with five mice per group. The dashed lines denote the corresponding thresholds for each fecal protein level (mean + 2SD of all mice in the NC [normal control] group). (F) Comparison of the maximum DSS (dextran sulfate sodium) to NC ratio and the corresponding effect size for candidate fecal proteins. $^{*}p < 0.05$, $^{**}p < 0.01$, $^{***}p < 0.001$, and $^{****}p < 0.0001$.

3.5 | Distribution and expression of the selected proteins in colon tissue

Distribution of complement C3, FN, and MUC2 in mouse colon tissue was observed via immunofluorescence (Figure 5A). In controls, clear FN and MUC2 fluorescence was observed along the colon structure, whereas C3 expression was relatively weak. Unlike their early elevation in feces, a delayed significant increase ($p < 0.05$) in tissue C3 and FN levels was observed from days 5 to 7 post-DSS treatment (Figure 5B,C). Meanwhile, MUC2 fluorescence gradually decreased over time (Figure 5D), exhibiting a strong negative correlation with DAI ($r = -0.7638$, $p < 0.0001$) (Figure S2). Importantly, on day 7, substantial C3 and FN signals were observed within the intestinal lumen, providing direct evidence for their measurement in fecal samples.

4 | DISCUSSION

In recent years, extensive research has focused on discovering efficient biomarkers for UC. Among these, FC has emerged as the most clinically valuable. However, more candidates are needed to better predict disease risk and reflect the underlying biology. In this study, we established a UC mouse model and identified two promising experimental candidates, namely fecal C3 and FN. Our results suggest that fecal C3 and FN respond earlier than FC after DSS treatment. They also exhibited a greater magnitude of increase and a larger effect size. Moreover, fecal C3 exhibited a stronger correlation with disease activity than FC. These results highlight their potential as fecal biomarkers to monitor UC disease activity.

The complement system is an important part of the innate immune system, participating in host immune defense and inflammatory responses. Recent studies have revealed the presence of an endogenous complement system in the gut.[15] Specifically, stromal cells within intestinal lymphoid follicles are a major source of luminal C3, and its concentration is significantly elevated during enteric infection in mice.[16] In this study, we also observed elevated C3 levels in colonic tissues and feces; differently, this was identified in DSS-induced UC mice. Therefore, we propose that the complement system is activated not only in enteric infection but also in UC and other noninfectious intestinal inflammation. Activated complement components could be secreted into the mucous layer and diffuse into the intestinal lumen, as observed in our immunofluorescence results. Moreover, in addition to complement C3, we observed significant enrichment of multiple other complement components (CFH, CFB, C4b, etc.) in the DSS group. KEGG analysis also revealed that a number of differential proteins were clustered within the complement activation pathway.

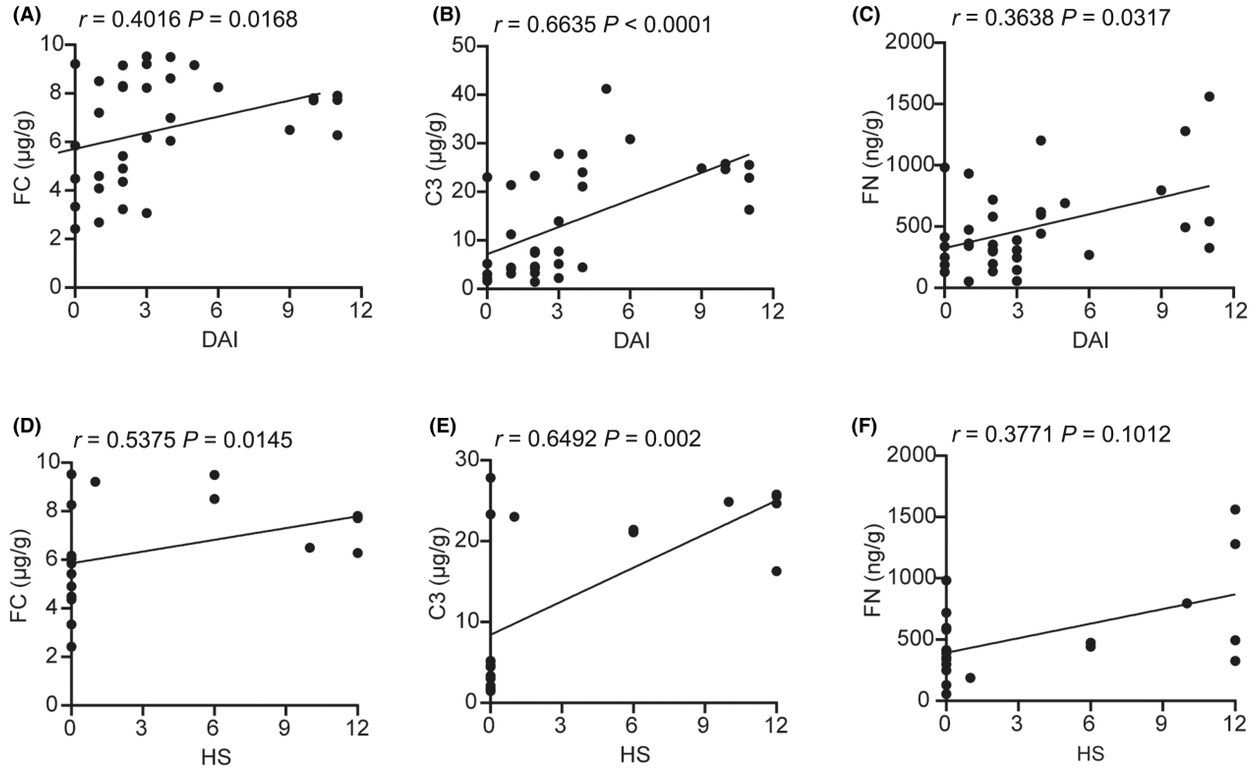

FIGURE 4 Correlation analysis of candidate protein levels with disease severity. (A–C) Correlation analysis of DAI (disease activity index) with FC (fecal calprotectin), C3 (component 3), and FN (fibronectin). Each point denotes an individual mouse ($N = 35$). (D–F) Correlation analysis of histopathological scores (HS) with FC, C3, and FN. Each point denotes an individual mouse ($N = 20$).

Using a multi-timepoint independent cohort design, we analyzed changes in fecal C3 levels across different stages of UC progression. In the DSS group, fecal C3 was significantly elevated compared to controls, starting as early as day 1. This finding suggests that the complement system may be activated at a very early stage of intestinal inflammation. Biologically, this observation is highly reasonable because complement activation constitutes an early event in the inflammatory cascade.[23] Upon exposure to stimuli like tissue damage or infection, the complement system is rapidly activated. This activation produces effector molecules, including the anaphylatoxins C3a and C5a, which are potent guides for neutrophil migration to inflammation sites.[24,25]

FN also exhibited a significant increase after DSS treatment on day 1. It is a core component of the ECM and contributes to intestinal barrier function by maintaining the integrity of the ECM.[26] In a recent study, researchers established a *Salmonella enterica* infection model in mice to study tissue-layer-specific ECM changes during inflammation.[20] They observed that FN fibers exhibited tension loss and progressive relaxation in both the intestinal smooth muscles and mucosa of infected mice. In our study, immunofluorescence revealed substantial FN signals in the intestinal lumen contents of UC mice, and this finding is consistent with the previous finding. The elevated fecal FN may be attributed to two possible mechanisms during active inflammation. On one hand, mucosal barrier disruption leads to passive leakage of FN. On the other hand, the host actively upregulates FN synthesis as an important component of the wound healing response. Additionally, researchers found that FN participates in the migration and adhesion of inflammatory cells (e.g., neutrophils and lymphocytes) to the site of inflammation via binding to integrin receptors on the cell surface.[27,28] In our proteomic analysis results, we observed a significant enrichment of both FN and integrins in the DSS group, which may be attributed to this mechanism.

We measured MUC2 levels in mouse feces. The results suggest only a transient increase in the DSS-treated mice in the early stage. We propose that during early UC, goblet cells not only remained intact but also mounted a compensatory upregulation of mucin production in response to inflammatory stress. However, after prolonged DSS exposure, they sustained severe damage; their subsequent decline in number caused a significant reduction in mucin production. Consequently, the early increase in fecal MUC2 was only transient.

This study has several limitations. First, our findings are based on a mouse model of acute colitis induced by a single concentration (3%) of DSS. Whether a lower DSS concentration would still elicit an early response of fecal C3 and FN remains to be investigated. Second, housing mice individually throughout the experiment may have induced additional stress, which could potentially affect disease progression. Third, previous studies using DSS-induced colitis models have reported that male mice often exhibit more severe histological damage compared to females, suggesting a biological impact of sex in this model, although results are conflicting across studies.[29] We chose female mice for their attenuated colitis phenotype, facilitating the identification of biomarkers that are sensitive to subtle fluctuations in disease activity. Future validation in

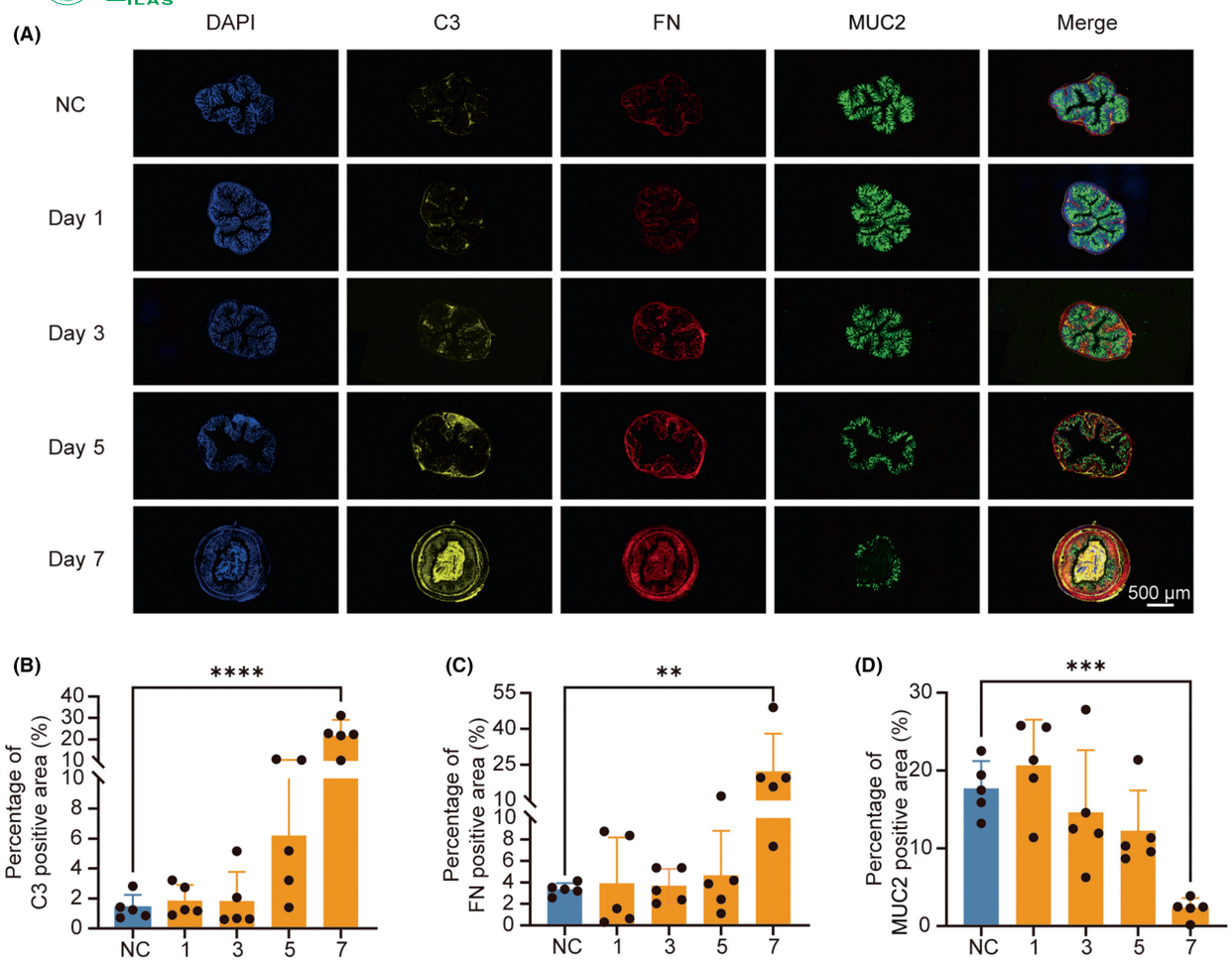

FIGURE 5 Immunofluorescence of the candidate proteins in colon tissue. (A) Distribution of C3 (component 3), FN (fibronectin), and MUC2 (mucin-2) in colon tissues from control and DSS (dextran sulfate sodium)–treated mice on days 1, 3, 5, and 7. (B–D) Proportion of the fluorescent-positive area of C3, FN, and MUC2 relative to the total colon area in mouse colon tissue. Blue indicates the NC (normal control) group, and orange denotes the DSS group on days 1, 3, 5, and 7. Each point denotes an individual mouse. $^{**}p < 0.01$, $^{***}p < 0.001$, and $^{****}p < 0.0001$.

human cohorts, accounting for sex as a biological variable, is essential. Fourth, although we performed initial validation of the ELISA kits used for C3 and FN quantifications, their accurate reliability for fecal samples necessitates more systematic evaluation. Fifth, fecal C3 and FN may lack disease specificity, a limitation shared by FC.[6] Finally, the translational potential of these proteins awaits validation in other types of colitis and, crucially, in human cohorts.

5 | CONCLUSION

In summary, this study demonstrated elevated levels of fecal C3 and FN in a DSS-induced UC mouse model. Importantly, fecal C3 exhibited a stronger correlation with disease activity than the clinically used FC. These results highlight the potential of fecal C3 and FN as promising biomarkers for monitoring UC disease activity, which requires further validation in other colitis models and human cohorts.

AUTHOR CONTRIBUTIONS

Yangyun Guo: Formal analysis; investigation; methodology; visualization; writing – original draft. **Ziheng Yan:** Methodology. **Jingyu Ye:** Methodology. **Ruifu Yang:** Funding acquisition; writing – review and editing. **Yajun Song:** Methodology; supervision; writing – review and editing. **Hui Yue:** Supervision; writing – review and editing. **Yong Zhao:** Conceptualization; formal analysis; project administration; writing – original draft; writing – review and editing.

FUNDING INFORMATION

This study was supported by the National Natural Science Foundation of China (32394054).

CONFLICT OF INTEREST STATEMENT

The authors declare no potential conflicts of interest with respect to the research, authorship, and/or publication of this article.

DATA AVAILABILITY STATEMENT

The data that support the findings of this study are available in the Supporting Information of this article. The mass spectrometry proteomics data have been deposited in the iProX under dataset identifier PXD075187.

ETHICS STATEMENT

All animal experiments were approved by the Academy of Military Medical Sciences and strictly adhered to animal ethics guidelines (approval no.: IACUC-DWZX-2025-006).

ORCID

Yong Zhao https://orcid.org/0000-0003-1648-4823

REFERENCES

1. Rubin DT, Ananthakrishnan AN, Siegel CA, Barnes EL, Long MD. ACG clinical guideline update: ulcerative colitis in adults. *Am J Gastroenterol*. 2025;120(6):1187-1224. doi:10.14309/ajg.0000000000003463
2. Rubin DT, Ananthakrishnan AN, Siegel CA, Sauer BG, Long MD. ACG clinical guideline: ulcerative colitis in adults. *Am J Gastroenterol*. 2019;114(3):384-413. doi:10.14309/ajg.0000000000000152
3. Pabla BS, Schwartz DA. Assessing severity of disease in patients with ulcerative colitis. *Gastroenterol Clin N Am*. 2020;49(4):671-688. doi:10.1016/j.gtc.2020.08.003
4. Ribeiro da Silva RAV, Genaro LM, Lahan-Martins D, Leal RF, Ayrizono MLS. Comparison between fecal calprotectin and magnetic resonance enterography in ileal Crohn's disease for activity disease assessment: a systematic review. *Transl Gastroenterol Hepatol*. 2025;10:73. doi:10.21037/tgh-24-159
5. Caron B, Sequier L, Dignass A, et al. Management of patients with ulcerative proctitis: a global survey. *Dig Dis Sci*. 2025;71:1416-1424. doi:10.1007/s10620-025-09538-2
6. Murray J, Kok KB, Ayling RM. Fecal calprotectin in gastrointestinal disease. *Clin Chem*. 2023;69(7):699-710. doi:10.1093/clinchem/hvad051
7. Selvakumar B, Samsudin R. Intestinal barrier dysfunction in inflammatory bowel disease: pathophysiology to precision therapeutics. *Inflamm Bowel Dis*. 2025;31:3450-3464. doi:10.1093/ibd/izaf225
8. Lee SH, Lopes E, Colombel JF, Ungaro R. Identifying potential targets for the interception of inflammatory bowel disease: toward precision prevention. *Inflamm Bowel Dis*. 2025;31(Supplement_2):S51-S60. doi:10.1093/ibd/izaf168
9. Alsoud D, Vermeire S, Verstockt B. Biomarker discovery for personalized therapy selection in inflammatory bowel diseases: challenges and promises. *Cur Res Pharmacol Drug Dis*. 2022;3:100089. doi:10.1016/j.crphar.2022.100089
10. Harder BJ, Lekkerkerker AN, Casavant EP, et al. Comprehensive profiling of the human fecal proteome from IBD patients with DIA-MS enables evaluation of disease-relevant proteins. *Proteomics Clin Appl*. 2024;18(5):e2300075. doi:10.1002/prca.202300075
11. Nowak JK, Kalla R, Satsangi J. Current and emerging biomarkers for ulcerative colitis. *Expert Rev Mol Diagn*. 2023;23(12):1107-1119. doi :10.1080/14737159.2023.2279611
12. Chassaing B, Srinivasan G, Delgado MA, Young AN, Gewirtz AT, Vijay-Kumar M. Fecal lipocalin 2, a sensitive and broadly dynamic non-invasive biomarker for intestinal inflammation. *PLoS One*. 2012;7(9):e44328. doi:10.1371/journal.pone.0044328
13. Zollner A, Schmiderer A, Reider SJ, et al. Faecal biomarkers in inflammatory bowel diseases: calprotectin versus lipocalin-2-a comparative study. *J Crohns Colitis*. 2021;15(1):43-54. doi:10.1093/ecco-jcc/jjaa124
14. Kemper C, Ferreira VP, Paz JT, Holers VM, Lionakis MS, Alexander JJ. Complement: the road less traveled. *J Immunol (Baltimore, Md: 1950)*. 2023;210(2):119-125. doi:10.4049/jimmunol.2200540
15. Tian X, Zhang L, Qian X, et al. Gut complement system: a new frontier in microbiota-host communication and intestinal homeostasis. *J Clin Invest*. 2025;135(19):e188349. doi:10.1172/jci188349
16. Wu M, Zheng W, Song X, et al. Gut complement induced by the microbiota combats pathogens and spares commensals. *Cell*. 2024;187(4):897-913.e18. doi:10.1016/j.cell.2023.12.036
17. Patten J, Wang K. Fibronectin in development and wound healing. *Adv Drug Deliv Rev*. 2021;170:353-368. doi:10.1016/j.addr.2020.09.005
18. Qin Z, Wang R, Zhang Y. Dual roles of complement in ulcerative colitis: insights from clinical studies and animal research. *Eur J Med Res*. 2025;30(1):1234. doi:10.1186/s40001-025-03400-x
19. Kolachala VL, Bajaj R, Wang L, et al. Epithelial-derived fibronectin expression, signaling, and function in intestinal inflammation. *J Biol Chem*. 2007;282(45):32965-32973. doi:10.1074/jbc.M704388200
20. Rappold R, Kalogeropoulos K, La Regina G, Auf dem Keller U, Slack E, Vogel V. Relaxation of mucosal fibronectin fibers in late gut inflammation following neutrophil infiltration in mice. *NPJ Biol Phys Mech*. 2025;2(1):4. doi:10.1038/s44341-024-00006-y
21. Hansson GC. Mucus and mucins in diseases of the intestinal and respiratory tracts. *J Intern Med*. 2019;285(5):479-490. doi:10.1111/joim.12910
22. Shin JH, Bozadjieva-Kramer N, Seeley RJ. Reg3γ: current understanding and future therapeutic opportunities in metabolic disease. *Exp Mol Med*. 2023;55(8):1672-1677. doi:10.1038/s12276-023-01054-5
23. Zarantonello A, Revel M, Grunenwald A, Roumenina LT. C3-dependent effector functions of complement. *Immunol Rev*. 2023;313(1):120-138. doi:10.1111/imr.13147
24. Peng Q, Li K, Sacks SH, Zhou W. The role of anaphylatoxins C3a and C5a in regulating innate and adaptive immune responses. *Inflamm Allergy Drug Targets*. 2009;8(3):236-246. doi:10.2174/187152809788681038
25. Sacks SH. Complement fragments C3a and C5a: the salt and pepper of the immune response. *Eur J Immunol*. 2010;40(3):668-670. doi:10.1002/eji.201040355
26. Biancheri P, Di Sabatino A, Corazza GR, MacDonald TT. Proteases and the gut barrier. *Cell Tissue Res*. 2013;351(2):269-280. doi:10.1007/s00441-012-1390-z
27. Koivisto L, Bi J, Häkkinen L, Larjava H. Integrin αvβ6: structure, function and role in health and disease. *Int J Biochem Cell Biol*. 2018;99:186-196. doi:10.1016/j.biocel.2018.04.013
28. Sutherland TE, Dyer DP, Allen JE. The extracellular matrix and the immune system: a mutually dependent relationship. *Science*. 2023;379(6633):eabp8964. doi:10.1126/science.abp8964
29. Tshikudi DM, Bernstein CN, Mishra S, Ghia JE, Armstrong HK. Influence of biological sex in inflammatory bowel diseases. *Nat Rev Gastroenterol Hepatol*. 2025;22(6):415-437. doi:10.1038/s41575-025-01038-y

SUPPORTING INFORMATION

Additional supporting information can be found online in the Supporting Information section at the end of this article.

How to cite this article: Guo Y, Yan Z, Ye J, et al. Identification and validation of fecal complement component 3 and fibronectin as potential biomarkers for monitoring disease activity in ulcerative colitis based on a mouse model. *Anim Models Exp Med*. 2026;9:1292-1301. doi:10.1002/ame2.70233